



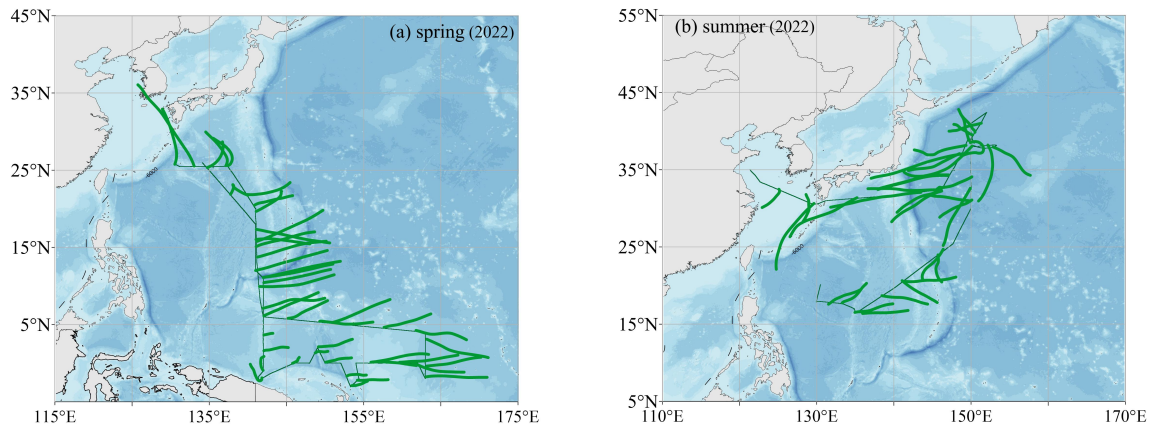
*Supplement of*

## **Biogenically driven marine organic aerosol production over the West Pacific Ocean**

**Yujue Wang et al.**

*Correspondence to:* Yujue Wang (wangyujue@ouc.edu.cn) and Wei Xu (wxu@iue.ac.cn)

The copyright of individual parts of the supplement might differ from the article licence.



25

**Figure S1** The 24-hr back trajectories of air masses during the cruises in (a) spring and (b) summer.

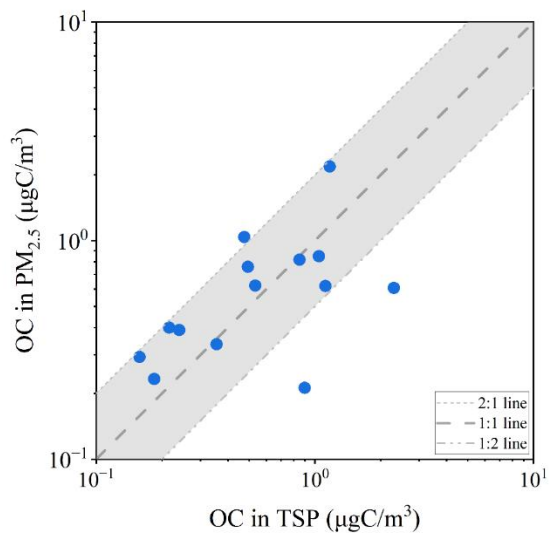
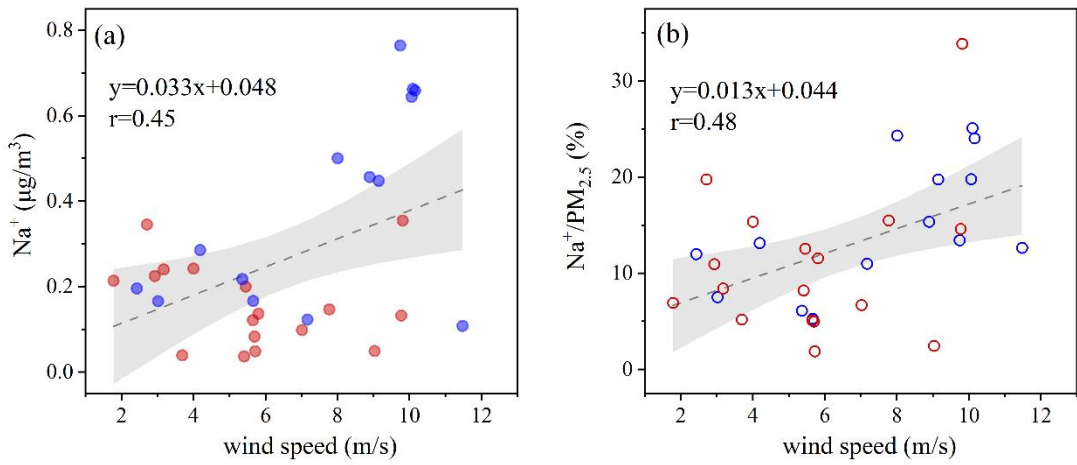
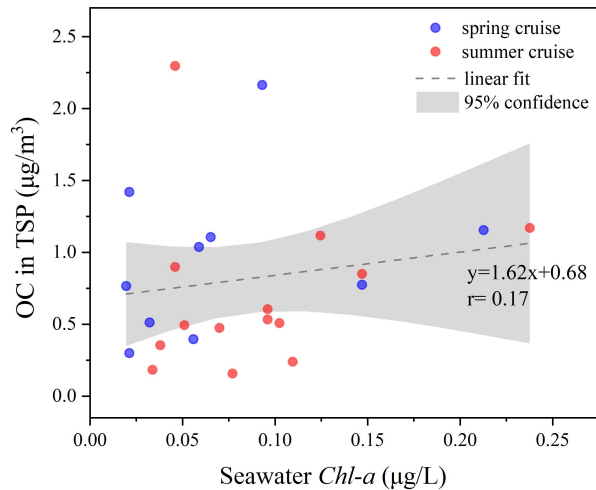


**Figure S2** Comparison of the OC concentrations in the PM<sub>2.5</sub> and the TSP samples during the spring observation (Cruise I)



30

**Figure S3** The variation of  $\text{Na}^+$  concentration and  $\text{Na}^+/\text{PM}_{2.5}$  as a function of the wind speed during the cruises. The data obtained during the spring Cruise I is in blue, and the data during the summer Cruise II is in red.



35

**Figure S4** Scatter plot of the OC concentration in the collected TSP samples and seawater  $\text{Chl-a}$  during the cruises.

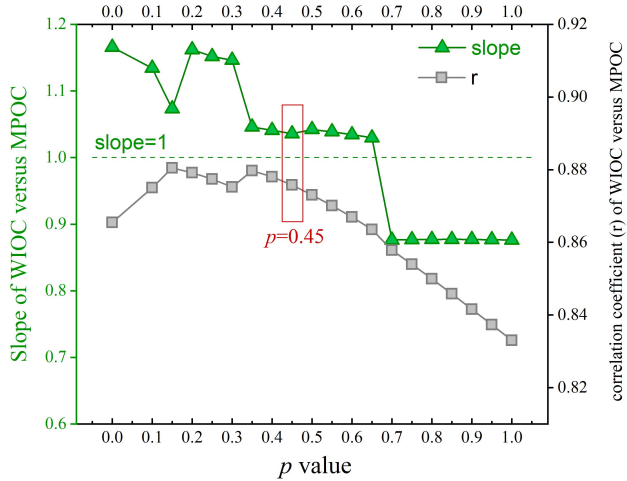


**Figure S5** The variations of the fitting line slopes and correlation coefficients (r) of WIOC and estimated MPOC, using Eq. 3 with the  $p$  value changing from 0–1.

40

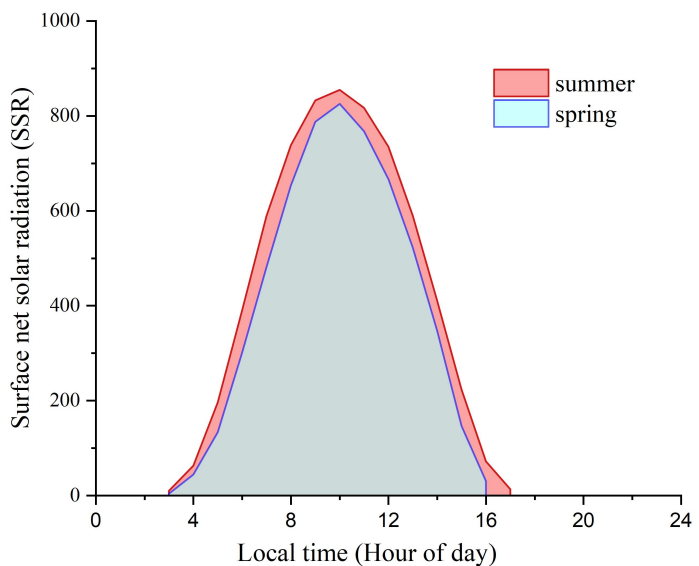


**Figure S6** Diurnal variation of the surface net solar radiation (SSR) within the 15°N–20°N during the spring and the summer cruises.

45

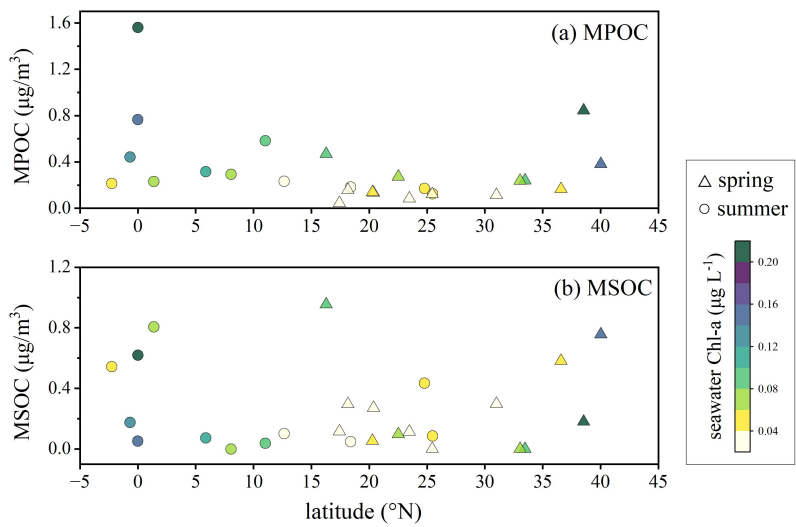


**Figure S7** Spatial distribution of the estimated MPOC and MSOC concentrations. The data is colored by the corresponding seawater *Chl-a* concentrations.

50

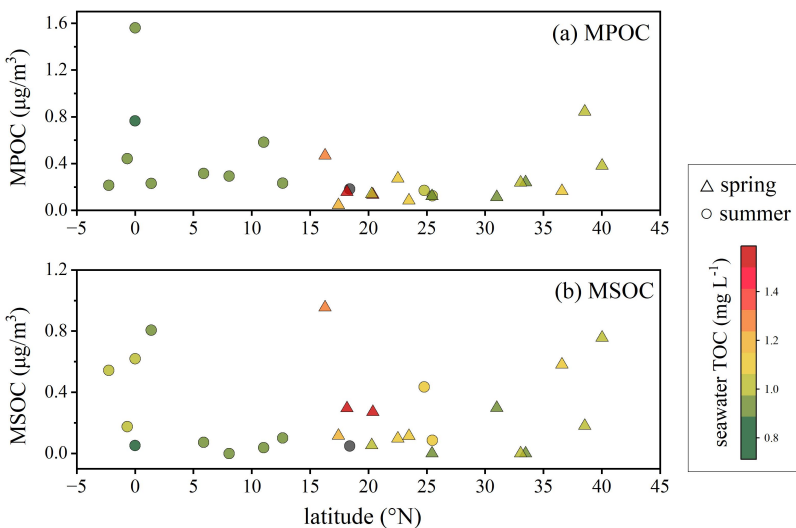
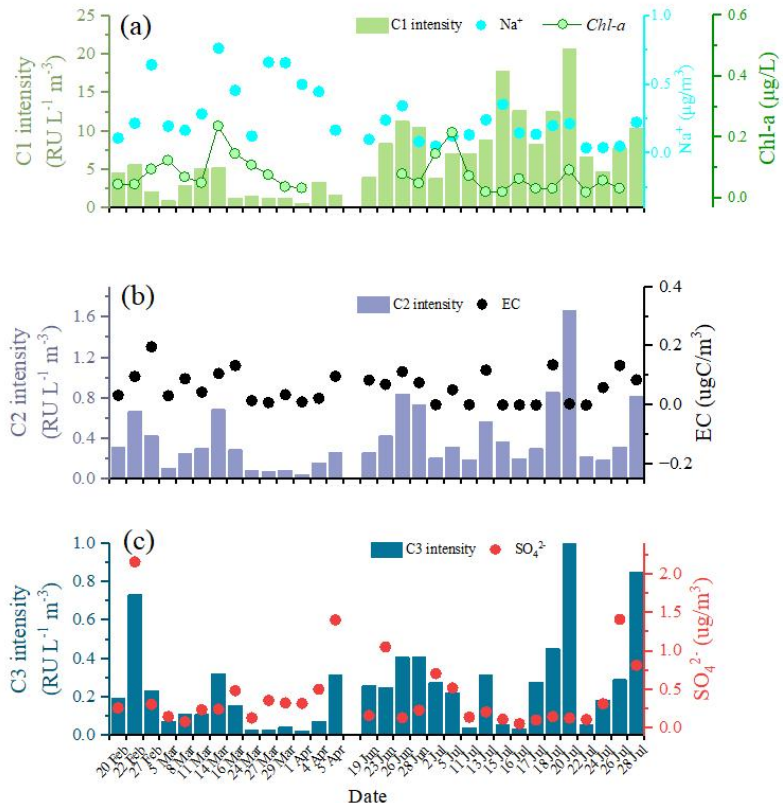


**Figure S8** Spatial distribution of the estimated MPOC and MSOC concentrations. The data is colored by the corresponding seawater TOC concentrations.



55

**Figure S9** Variations of fluorescence component intensity identified by three-component solutions based on PARAFAC model analysis and related aerosol components: (a) C1,  $\text{Na}^+$ , and  $\text{Chl-a}$ , (b) C2 and EC, (c) C3 and  $\text{SO}_4^{2-}$ .

60